

Supplementary Materials for

Na⁺-induced structural transition of MotPS for stator assembly of the *Bacillus* flagellar motor

Naoya Terahara, Noriyuki Kodera, Takayuki Uchihashi, Toshio Ando, Keiichi Namba, Tohru Minamino

Published 1 November 2017, *Sci. Adv.* **3**, eaao4119 (2017)

DOI: 10.1126/sciadv.aao4119

The PDF file includes:

- fig. S1. Primary structures of MotB and its homologs, MotS and PomB.
- fig. S2. Effect of Na⁺ concentrations on motor rotation of the flagellar motor in wild-type *Bacillus* cells expressing both MotAB and MotPS.
- fig. S3. Purification of His₆-tagged MotPS by size exclusion chromatography.
- fig. S4. Comparison of simulated AFM images of the MotB_C and the MotA tetramer with experimental image of the MotPS complex.
- fig. S5. Two distinct conformations of the PGB domain of MotS.
- fig. S6. Motility of *motS* mutants.
- table S1. Rotational speed and torque of the wild-type motor.
- table S2. Speed fluctuations of the wild-type, MotAB, and MotPS motor.
- Legends for movies S1 to S8

Other Supplementary Material for this manuscript includes the following:

(available at advances.sciencemag.org/cgi/content/full/3/11/eaao4119/DC1)

- movie S1 (.mov format). Real-time imaging of wild-type MotPS by HS-AFM.
- movie S2 (.mov format). Typical HS-AFM imaging of wild-type MotPS in buffer containing 150 mM NaCl.
- movie S3 (.mov format). Typical HS-AFM imaging of MotPS_{Δperi} in buffer containing 150 mM NaCl.
- movie S4 (.mov format). Typical HS-AFM imaging of MotPS_{B-PGB} in buffer containing 150 mM NaCl.
- movie S5 (.mov format). Real-time imaging of a disorder-to-order transition of MotPS with an increase in the concentration of NaCl.

- movie S6 (.mov format). Real-time imaging of a order-to-disorder transition of MotPS with a decrease in the concentration of NaCl.
- movie S7 (.mov format). Typical HS-AFM imaging of MotPS_{Δplug} in buffer containing 150 mM NaCl.
- movie S8 (.mov format). Typical HS-AFM imaging of MotPS_{D30A} in buffer containing 150 mM NaCl.

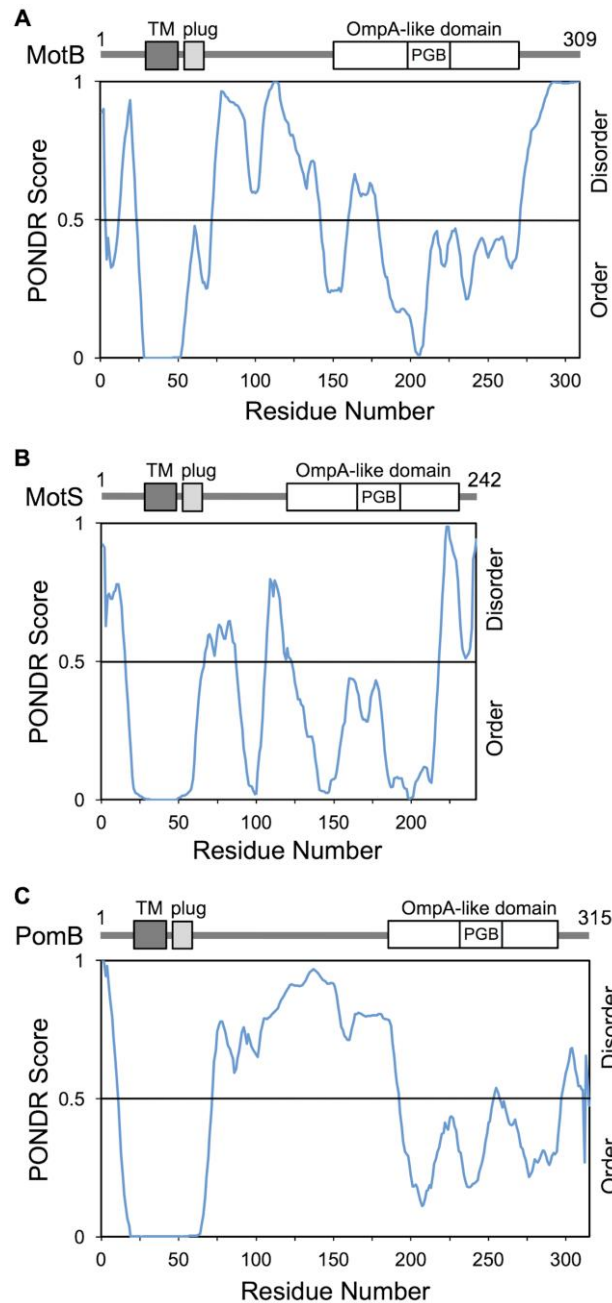


fig. S1. Primary structures of MotB and its homologs, MotS and PomB. (A) *Salmonella* MotB. MotB contains a single transmembrane helix (indicated as TM) and a C-terminal periplasmic region including a plug segment (indicated as plug), which suppresses the proton channel activity of the MotAB complex prior to stator assembly around a rotor, and an OmpA-like domain with a putative peptidoglycan-binding motif (indicated as PGB), which is responsible for anchoring of the MotAB complex to the peptidoglycan layer. (B) *Bacillus subtilis* MotS. (C) *Vibrio alginolyticus* PomB. Prediction of intrinsically disordered (ID) regions of MotB, MotS and PomB by PONDNR program, which is a program for prediction of ID regions of proteins (<http://www.pondr.com>). PONDNR profiles were made by the scores that were calculated on the basis of the primary sequence. Regions with residues having PONDNR scores exceeding a threshold of 0.5 are predicted to be disordered. The N-terminal cytoplasmic and C-terminal periplasmic regions of MotB, MotS and PomB are predicted to contain ID regions.

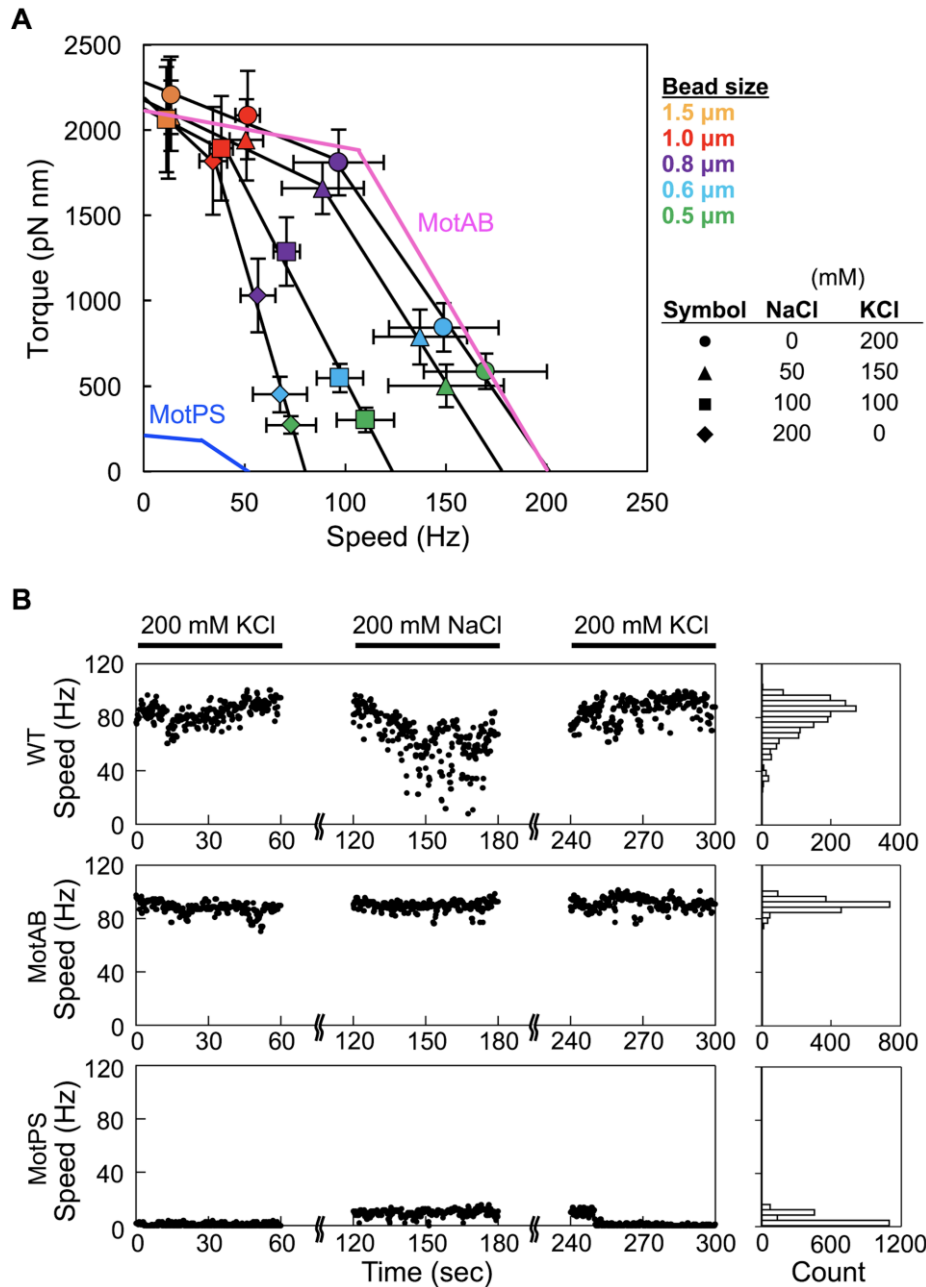


fig. S2. Effect of Na^+ concentrations on motor rotation of the flagellar motor in wild-type *Bacillus* cells expressing both MotAB and MotPS. (A) Torque-speed relationship of the wild-type motor under 200 mM K^+ (circle), 150 mM K^+ plus 50 mM Na^+ (triangle), 100 mM K^+ plus 100 mM Na^+ (square) or 200 mM Na^+ (diamond) condition. Rotation measurements were carried out at room temperature by tracking the positions of 1.5 μm (orange), 1.0 μm (red), 0.8 μm (purple), 0.6 μm (cyan) or 0.5 μm (green) polystyrene beads attached to the sticky filament of the flagellar motor. At least twenty individual beads of each size were measured (table S1). The torque-speed curve of the flagellar motor consists of two regimes: a high-load, low-speed regime and a low-load, high-speed regime (3) and so the curve was fitted by two straight lines with an intersection at the speed of 0.8 μm (circle and triangle) and 1.0 μm bead (square and diamond). The torque-speed curves of the MotAB and MotPS motors, which have been published previously (10), are shown by magenta and blue lines, respectively. The number of active stator units in the MotAB and MotPS motors are estimated to ten and one, respectively, and hence the stall torque produced

by the MotPS motor was about 10 times lower than that by the MotAB motor (10). **(B)** Reversibility of the effect of Na^+ ions on the rotation rate of the wild-type motor. Rotation rates were measured by tracking the position of a $0.8 \mu\text{m}$ bead attached to the sticky filament of the wild-type (first panel), MotAB (second panel) and MotPS motors (third panel) in motility buffer containing 200 mM KCl. The motility buffer was changed to that containing 200 mM NaCl, and then replaced the buffer by the original one containing 200 mM KCl. Traces and speed histograms of the wild-type, MotAB and MotPS motors are shown.

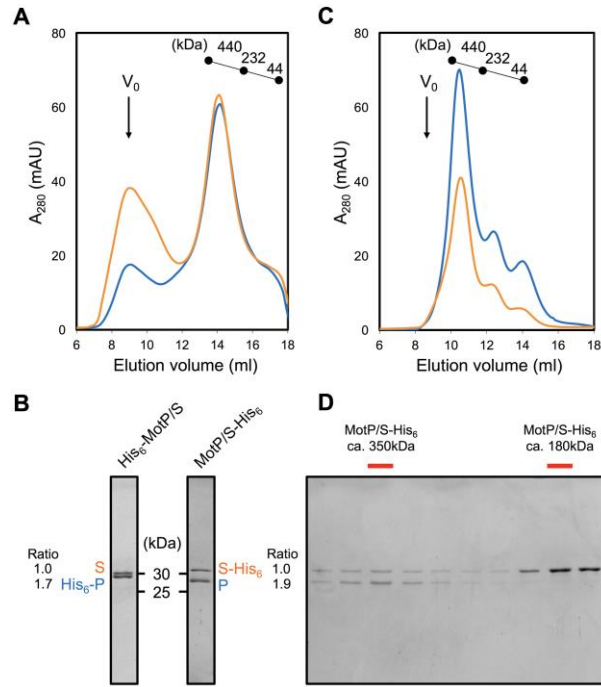


fig. S3. Purification of His₆-tagged MotPS by size exclusion chromatography. (A) Size exclusion chromatography (SEC) elution profiles of His₆-MotP/S (His₆-MotP/S) (orange) and MotP/S-His₆ (MotP/S-His₆) (blue) in the presence of DMNG. V₀ indicates a position of void volume. A standard curve was made from the elution volume of main peaks of ferritin (440 kDa), catalase (232 kDa) and ovalbumin (44 kDa). (B) SDS-PAGE analysis of peak fractions shown in (A). Relative band intensities of His₆-MotP and MotP in His₆-MotP/S (right) and MotP/S-His₆ (left) complex were normalized for those of MotS and MotS-His₆, respectively. These data were the average of five independent purification samples. (C) SEC elution profiles of amphipol-treated His₆-MotP/S (orange) and MotP/S-His₆ (blue). (D) SDS-PAGE analysis of elution peak fractions of MotP/S-His₆ complex shown in (C). An elution peak of the MoPS complex indicated that an apparent molecular mass of the complex was about 350 kDa. Since amphipol A8-35, which serves as a stabilizer of transmembrane proteins in solution, covers transmembrane helices of the MotPS complex, relative band intensities of MotP and MotS in the MotPS complex allowed us to roughly estimate that four copies of MotP and two copies of MotS form a Na⁺ channel in a manner similar to the MotAB proton channel (Fig. 2A).

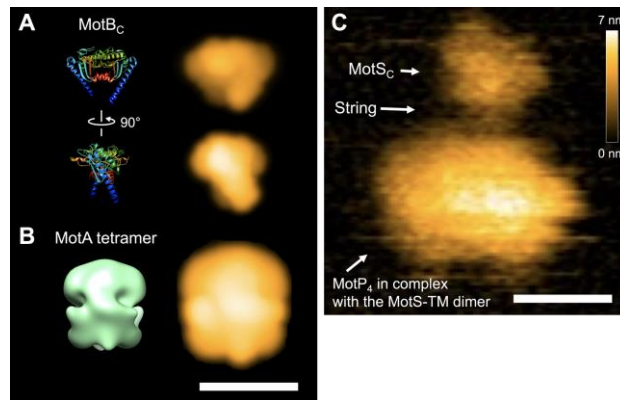


fig. S4. Comparison of simulated AFM images of the MotB_C and the MotA tetramer with experimental image of the MotPS complex. (A) Simulated AFM images constructed from the crystal structure of MotB_C (PDB code: 2ZVY). Two different views are shown. MotB_C is relatively flat in shape so that a 90° rotation from the orientation shown in the upper panel increases the height from 5.3 nm to 6.7 nm. Scale bar indicates 10 nm. (B) Simulated AFM image constructed from the electron density map of the MotA tetramer obtained by electron microscopy with negative staining and single particle image analysis (25). (C) Experimental HS-AFM image of the wild-type MotPS complex shown in Fig. 2C. Color bar indicates a range of particle heights (nm).

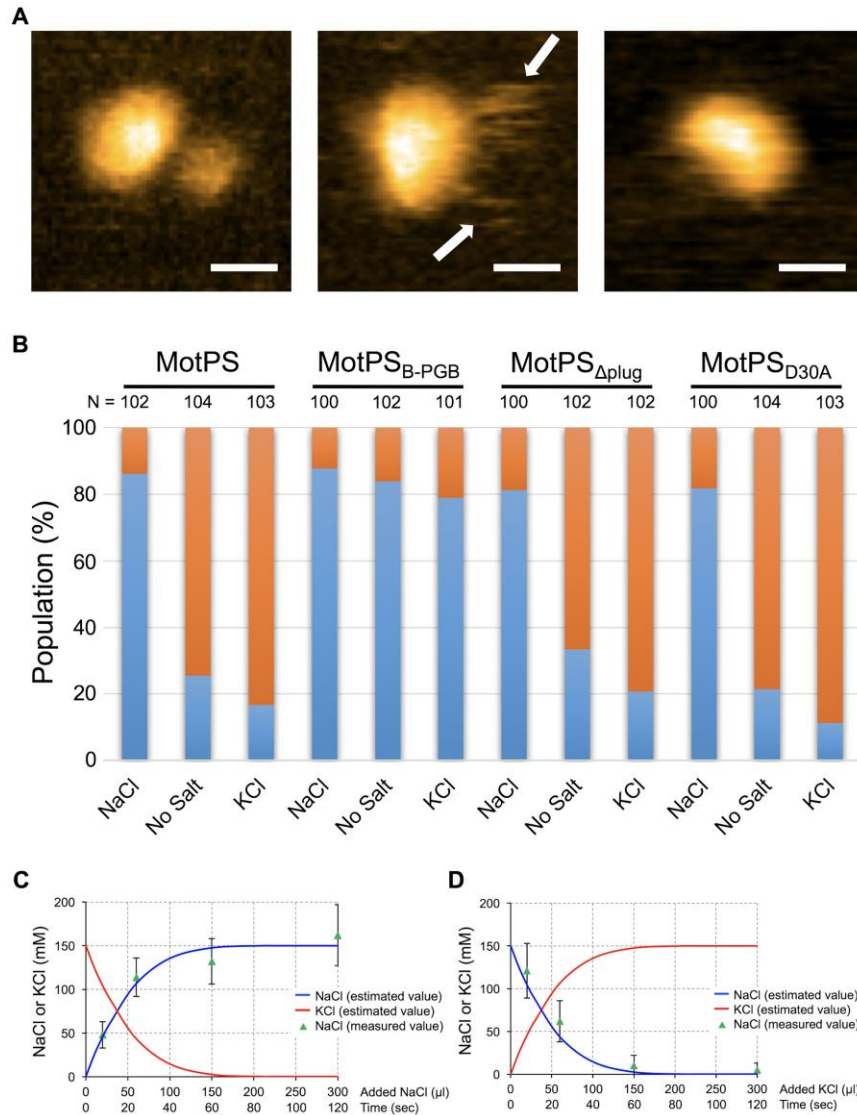


fig. S5. Two distinct conformations of the PGB domain of MotS. (A) Typical HS-AFM images of wild-type MotPS. The PGB domain of MotS_C adopted two distinct, compactly folded (left) and unfolded conformations (middle; two arrows indicate the unfolded conformation of MotS_C). Several % of particles did not have the PGB domain of MotS (right). All images were recorded at 200 ms per frame in a scanning area of 50 nm × 50 nm with 150 pixels × 150 pixels. Scale bar shows 10 nm. (B) Populations of the PGB domains adopting the folded (light blue) and unfolded (orange) conformations in the presence of 150 mM NaCl or KCl. The number of particles of MotPS, MotPS_{B-PGB}, MotPS_{Δplug} and MotPS_{D30A} in each condition (indicated as N), which we analyzed, are shown. (C, D) Estimation of NaCl (blue) and KCl (red) concentrations in a buffer solution when gradually exchanging the salt from 150 mM KCl to 150 mM NaCl (C) or from 150 mM NaCl to 150 mM KCl (D) shown in Fig. 3A and B, respectively. Actual Na⁺ concentrations (green triangle) were measured by CoroNa Green. The mean and standard deviation of three independent measurements are shown.

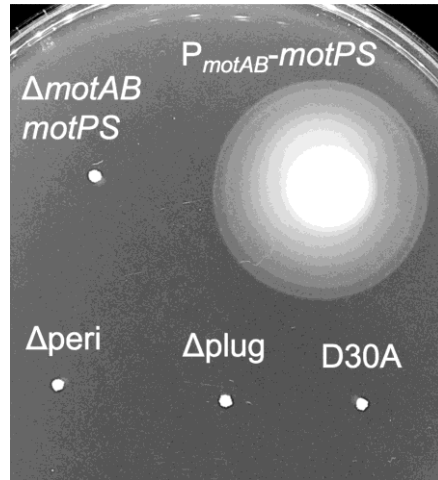


fig. S6. Motility of *motS* mutants. Motility assay of *B. subtilis* cells expressing wild-type MotPS or its mutant variants from the *motAB* promoter in soft agar plate. Plates were incubated at 37°C for 10 h.

table S1. Rotational speed and torque of the wild-type motor.

NaCl (mM)	KCl (mM)	Bead size (μm)	1.5	1.0	0.8	0.6	0.5
0	200	Speed (Hz)	14 ± 2	52 ± 8	97 ± 19	149 ± 25	169 ± 30
		Torque (pN nm)	$2,203 \pm 259$	$2,086 \pm 226$	$1,809 \pm 191$	841 ± 142	585 ± 103
		Number of motors	21	26	25	28	28
50	150	Speed (Hz)	14 ± 2	51 ± 8	89 ± 18	137 ± 22	153 ± 28
		Torque (pN nm)	$2,083 \pm 239$	$1,942 \pm 206$	$1,657 \pm 161$	786 ± 141	501 ± 123
		Number of motors	23	23	25	26	27
100	100	Speed (Hz)	11 ± 2	38 ± 7	71 ± 14	97 ± 18	110 ± 20
		Torque (pN nm)	$2,061 \pm 218$	$1,892 \pm 205$	$1,287 \pm 134$	546 ± 85	300 ± 72
		Number of motors	20	21	24	27	25
200	0	Speed (Hz)	12 ± 3	34 ± 7	57 ± 9	68 ± 13	73 ± 14
		Torque (pN nm)	$2,062 \pm 228$	$1,817 \pm 216$	$1,029 \pm 116$	449 ± 75	270 ± 52
		Number of motors	21	22	25	25	27

table S2. Speed fluctuations of the wild-type, MotAB, and MotPS motor.

Strain		200 mM KCl	200 mM NaCl	200 mM KCl
WT	ω_{av} (Hz)	83.8	65.8	86.3
	σ_{ω}	7.5	19.5	7.9
	$\sigma_{\omega}/\omega_{av}$	0.09	0.30	0.09
MotAB	ω_{av} (Hz)	88.1	89.9	91.6
	σ_{ω}	6.3	6.0	6.3
	$\sigma_{\omega}/\omega_{av}$	0.07	0.07	0.07
MotPS	ω_{av} (Hz)	-	9.8	-
	σ_{ω}	-	2.3	-
	$\sigma_{\omega}/\omega_{av}$	-	0.24	-

The average speed (ω_{av}), and standard deviation (σ_{ω}) in each condition were calculated as follows

$$\omega_{av} = \frac{N}{\sum_{k=1}^N \tau(k)}$$

$$\sigma_{\omega} = \sqrt{\frac{\sum_{k=1}^N \{\omega(k) - \omega_{av}\}^2 \tau(k)}{\sum_{k=1}^N \tau(k)}}$$

movie S1. Real-time imaging of wild-type MotPS by HS-AFM. Frame rate, 500 ms per frame (playback rate, 10 frames/sec). Scan area, 261 nm × 249 nm. Related to Fig. 2.

movie S2. Typical HS-AFM imaging of wild-type MotPS in buffer containing 150 mM NaCl. Frame rate, 100 ms per frame (playback rate, 15 frames/sec). Scan area, 44 nm × 42 nm. Related to Figs. 2 and 4A.

movie S3. Typical HS-AFM imaging of MotPS_{Δperi} in buffer containing 150 mM NaCl. Frame rate, 100 ms per frame (playback rate, 15 frames/sec). Scan area, 41 nm × 39 nm. Related to Fig. 2.

movie S4. Typical HS-AFM imaging of MotPS_{B-PGB} in buffer containing 150 mM NaCl. Frame rate, 100 ms per frame (playback rate, 15 frames/sec). Scan area, 50 nm × 50 nm. Related to Fig. 2.

movie S5. Real-time imaging of a disorder-to-order transition of MotPS with an increase in the concentration of NaCl. Frame rate, 250 ms per frame (playback rate, 12 frames/sec). Scan area, 35 nm × 34 nm. Related to Fig. 3A.

movie S6. Real-time imaging of a disorder-to-order transition of MotPS with a decrease in the concentration of NaCl. Frame rate, 250 ms per frame (playback rate, 12 frames/sec). Scan area, 38 nm × 39 nm. Related to Fig. 3B.

movie S7. Typical HS-AFM imaging of MotPS_{Δplug} in buffer containing 150 mM NaCl. Frame rate, 100 ms per frame (playback rate, 15 frames/sec). Scan area, 50 nm × 50 nm. Related to Figs. 2 and 4C.

movie S8. Typical HS-AFM imaging of MotPS_{D30A} in buffer containing 150 mM NaCl. Frame rate, 100 ms per frame (playback rate, 15 frames/sec). Scan area, 50 nm × 50 nm. Related to Figs. 2 and 4E.